

BULK HEATING AND SLENDER MAGNETIC LOOPS IN THE SOLAR CORONA

B.V. GUDIKSEN AND Å. NORDLUND
Draft version October 31, 2018

ABSTRACT

The heating of the solar corona and the puzzle of the slender high reaching magnetic loops seen in observations from the Transition Region And Coronal Explorer(TRACE) has been investigated through 3D numerical simulations, and found to be caused by the well observed plasma flows in the photosphere displacing the foot points of magnetic loops in a nearly potential configuration. It is found that even the small convective displacements cause magnetic dissipation sufficient to heat the corona to temperatures of the order of a million Kelvin. The heating is intermittent in both space and time—at any one height and time it spans several orders of magnitude, and localized heating causes transonic flows along field lines, which explains the observed non-hydrostatic stratification of loops that are bright in emission measure.

Subject headings: Sun: corona — Sun: magnetic fields — MHD — Sun: transition region

1. INTRODUCTION

The Sun has provided us with a problem that has puzzled researchers for many decades. The solar corona has a sustained temperature of the order of one million Kelvin, three orders of magnitude higher than the photosphere. On top of that the corona shows magnetic structures in the form of loops reaching high into the corona through several pressure scale heights while still being below the resolution limit of the best instruments available at the appropriate wavelengths. Even though several heating processes could be at work, with bulk heating largely independent of the mechanism creating the slender loops, both effects are concentrated around active regions, and there are therefore strong indications that they are related. If the bulk and loop heating mechanisms are actually the same, the heating mechanism must operate partly on scales smaller than the resolution limit of $1.0''$ (~ 725 km) of the TRACE instrument (Aschwanden et al. 2000) in order to explain the high reaching slender loops, and partly on scales comparable to the size of an active region. Both the bulk heating and the loops are believed to be related to magnetic processes, but identifying the main contributing effects has proven difficult.

Coronal active regions need a continuous thermal energy input of $10^6 - 10^7$ ergs $\text{cm}^{-2} \text{s}^{-1}$ in order to counter thermal conduction and X-ray losses at coronal temperatures. Several heating mechanisms have been proposed, among them wave dissipation, direct current (DC) dissipation, and nano-flares. Wave dissipation is only possible for Alfvén waves, since the other magneto-sonic wave modes are diffracted and dissipated by the strong wave speed gradient in the chromosphere region. To make Alfvén waves dissipate their energy in the corona is not easy and the physical requirements are hard to meet. Direct current dissipation is relatively easy to realize, but it has been unknown whether it is possible to induce enough current in the observed, nearly potential magnetic field configuration, and at the correct heights. Nano-flares have until recently been a promising candidate, but observations now seem to indicate that the power in the observed nano-flares is insufficient (Aschwanden et al. 2000; Parnell & Jubb 2000, and references therein).

The DC heating mechanism appears to be the most promising one. It was proposed 30 years ago (Parker 1972), and has received a lot of attention over the years (e.g. Parker 1972, 1983; Sturrock & Uchida 1981; van Ballegooijen 1986; Mikić

et al. 1989; Heyvaerts & Priest 1992; Longcope & Sudan 1994; Galsgaard & Nordlund 1996; Hendrix et al. 1996; Gomez et al. 2000, to mention just a few). These works have generally argued that the mechanism is feasible, but have been unable to actually demonstrate that it works, in the sense that it produces the right amount of heating, and the observed type of coronal structures. An important step forward was taken when Galsgaard & Nordlund (1996) and Hendrix et al. (1996) showed that the dissipation does not depend on, or depends only very weakly on the magnetic Reynolds number (or equivalently, the resolution of numerical experiments).

As pointed out by Aschwanden (2001) and others, it is necessary to deal with the correct geometry and stratification in order to verify or falsify a proposed mechanism. One cannot, for example, hope to reproduce the distribution of heating along the length of loops without representing the loop geometry reasonably correctly. In addition, since the main cooling mechanisms depend strongly on topology (for thermal conduction) and on density stratification (for radiative cooling), it is obvious that the question of coronal heating can only be answered by employing a sufficiently realistic setup.

We use a 3D magneto-hydro-dynamics (MHD) code (Nordlund & Galsgaard 1995) to simulate a typical scaled down active region, including a simple photospheric driving and starting with a potential field extrapolation from an MDI magnetogram, in order to investigate if the convective motions of the solar photosphere are sufficient to heat the corona through magnetic field line braiding. We conclude that even though the magnetic field remains not far from a potential field configuration, the convective driving is all that is needed to heat the corona and produce hot loops such as those seen in, e.g., the TRACE 171 Å filter, through a DC heating mechanism.

2. NUMERICAL PROCEDURES

The numerical code uses 6'th order differential operators and 5'th order translational operators on a staggered mesh to solve the fully compressible MHD equations. Radiative cooling (Kahn 1976) and Spitzer conductivity (Spitzer 1956) along the magnetic field are included in the energy equation.

The velocity field at the lower boundary is updated through a procedure that smoothly changes horizontal velocities for a given scale from one random pattern to another over a turn-over

time appropriate for each scale. The horizontal velocity pattern is generated from a velocity potential with randomly phased 2-D Fourier components, with amplitudes that follow a power law k^{-p} . The velocity power spectrum is then $P(k) \propto k^{3-2p}$, typical velocities at scales $1/k$ are $v(k) \propto \sqrt{kP(k)} \propto k^{2-p}$, and the corresponding turn-over times $\tau(k) = 1/kv(k) \propto k^{p-3}$.

We choose to set $p = 1$, which is consistent with observed super granulation and granulation turnover times; ~ 30 hours at scales ~ 30 Mm, and ~ 1000 s at scales ~ 3 Mm, respectively. A power spectrum $P(k) \propto k$ is also consistent with the large scale part of the power spectrum in well established simulations of convection on granular and meso granular scales (Stein & Nordlund 1998). At smaller scales the granulation velocity power deviates from $P(k) \propto k$, peaking at $k \sim 4-6$ Mm $^{-1}$ and decreasing at even larger k . These scales are, however, below the horizontal resolution of the present experiment.

We increased the velocity field amplitude by about a factor two, relative to the rms horizontal velocity from convection simulations, in order to counter the effects of our extended chromosphere and transition region (see Section 3). It remains to be seen if future simulations, with improved vertical and horizontal resolution, will be able to achieve similar results while using a properly normalized velocity power spectrum.

3. INITIAL CONDITIONS

The initial conditions were resolved on a uniform grid with 111 points in the vertical direction (x), including 11 “ghost zones”, and 100×100 grid points in the horizontal (periodic) directions (y, z). The grid spans a volume $30 \times 50 \times 50$ Mm 3 excluding ghost zones, giving a resolution of 0.3 Mm vertically and 0.5 Mm horizontally.

The requirements of having a high plasma beta ($\beta = P_{\text{gas}}/P_{\text{mag}}$) at the lower boundary, while at the same time reaching the much lower coronal pressures across a thin chromosphere, gives a resolution problem not easily solved on a uniform grid, and requires a compromise. We chose to extend the thickness of the “chromosphere” to about 4 Mm, in order to be able to cover the large change of pressure there with about one point per scale height.

This solution has the side effect that if the heating decreases exponentially with height (as seems to be the case; see Schrijver et al. 1999; Aschwanden, Schrijver & Alexander 2001; Aschwanden, Nightingale & Alexander 2000), we underestimate the heating. Our chromosphere is roughly 1.5 Mm thicker than the VAL models of the solar chromosphere (Vernazza, Avrett & Loeser 1981). The corresponding decrease of the heating is approximately compensated for by our increase in velocity driving amplitude.

The lower boundary and photosphere is kept at a constant temperature 8×10^3 K. The upper boundary is kept at the initial temperature (10^6 K) during the start-up phase. Thereafter a vanishing vertical derivative of temperature is assumed, thus enforcing a vanishing vertical component of the thermal conductive flux there.

The initial condition for the magnetic field is derived from a magnetogram of active region 9114, observed near disc center by TRACE and by the Michelson Doppler Imager (MDI) on the SOLar and Heliospheric Observatory (SOHO) on August 8, 2000. The original magnetogram was cropped at a perimeter chosen to intersect a minimum of magnetic field, and was then made periodic by taking a Fourier transform. The physical range of the observed active region was then scaled down from

~ 250 Mm to 50 Mm in order to fit in the computational domain, while still having magnetic structures on even the smallest scales. This was done because the details of the magnetic field are not terribly important, since we did not try to reenact the dynamics of AR9114 in particular. We are satisfied to have a reasonable realistic initial distribution of the magnetic field in our model, and aim rather at studying the generic behavior of active regions.

The initial magnetic field was obtained by making a potential extrapolation from the vertical magnetic field from the magnetogram. In the subsequent evolution, the magnetic field at the boundary evolves under the control of the random horizontal velocity field, specified as explained above. The vertical velocity is assumed to vanish at the boundary. The horizontal velocity field is divergence free by construction, so the evolution corresponds to moving the foot points of the magnetic field around, while conserving the magnetic flux density.

4. RESULTS

After an initial start-up phase the simulation evolves towards a quasi-stationary configuration with a hot tenuous corona with temperatures of the order a million K. The horizontally averaged temperature peaks at about 1.3 MK, about 6 Mm above the transition zone. Maximum temperatures ~ 4 MK are reached about 10 Mm above the transition zone, where the average temperature is ~ 1.1 MK (these are mentioned merely as examples—the detailed numbers are expected to vary between active regions).

The temperature, density, pressure, electric current density, and velocity all vary considerably across horizontal planes, but tend to vary much less dramatically along magnetic field lines.

The average density at a height of 10 Mm above the transition zone is $\sim 2 \times 10^{-15}$ g cm $^{-3}$, or about 10^9 atoms per cm $^{-3}$. The maximum density is typically 20–30 times higher; i.e., around $2-3 \times 10^{10}$ cm $^{-3}$. The large variation of density and temperature between magnetic field lines is the main cause of the appearance of loop-like structures in Fig. 2.

The chromosphere and transition region turn out to be of crucial importance, as predicted by Aschwanden (2001). The root mean square electric current decreases exponentially by almost three orders of magnitude in the lower chromosphere. There, the magnetic field is non-force-free, with a very intermittent Lorentz force that interacts with both gas pressure gradients and inertial forces.

In the upper chromosphere the magnetic field gradually becomes nearly force-free, and therefore the scale height of the J^2 distribution approaches that of B^2 (cf. Fig. 1). Even though there are large variations in horizontal planes, over which the current distribution is very intermittent, the height dependence of the root mean square electric current in the corona more or less follows that of the magnetic field, as is to be expected from a distribution with approximately “constant alpha” ($\alpha = \mathbf{J} \cdot \mathbf{B}/B^2$) along magnetic field lines.

In the transition region between the chromosphere and the corona the density and pressure scale heights rapidly change to much larger values. The average Joule dissipation thus decreases faster than the radiative cooling in the corona, and therefore the peak of the average temperature occurs low in the corona. The temperature structure from the transition region to the maximum of the temperature is mainly determined by heat conduction along magnetic field lines.

The average Joule dissipation, which balances the sum of

thermal conduction losses and radiation losses, increases monotonically with decreasing height, which makes it difficult to unambiguously define an average coronal heating rate. However, over the region in height where the temperature is larger than one million K, the average heating rate is $\sim 2 \cdot 10^6 \text{ erg cm}^{-2} \text{ s}^{-1}$.

The heating varies considerably over the horizontal plane, with much larger average rates in the immediate neighborhood of the active region patches of strong magnetic field (except right above the sunspot, where the heating rate is low). The heating rate in the 25% of the horizontal area that covers the central part of the active region is 2–3 times higher than the average over the whole model.

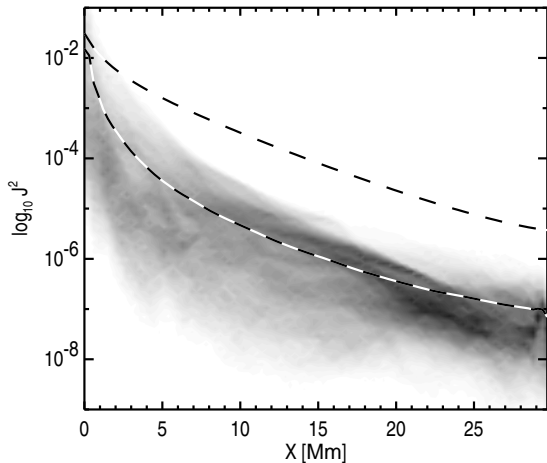


Fig. 1: Histogram of current density squared as a function of height. Dark colors are higher filling factor. The upper and lower dashed lines are the horizontal averages of the magnetic field strength squared and the Joule heating squared, respectively.

The Joule heating is plotted as a scatter histogram in Fig. 1. Although there is a relatively large scatter in the numerical values at each height, the horizontal average shows a smooth, roughly exponential height dependence. The magnetic dissipation thus indeed decreases roughly exponentially with height, as was proposed by Schrijver et al. (1999), and as was deduced from TRACE data by Aschwanden, Schrijver & Alexander (2001).

Note that the scale height of the heating empirically is found to increase with loop length; Aschwanden et al. (2000) report a ratio ~ 0.2 between the scale height and the loop length. Such an approximate proportionality should indeed be expected, if the heating is controlled by a roughly constant winding number from one loop end to another (Galsgaard & Nordlund 1996).

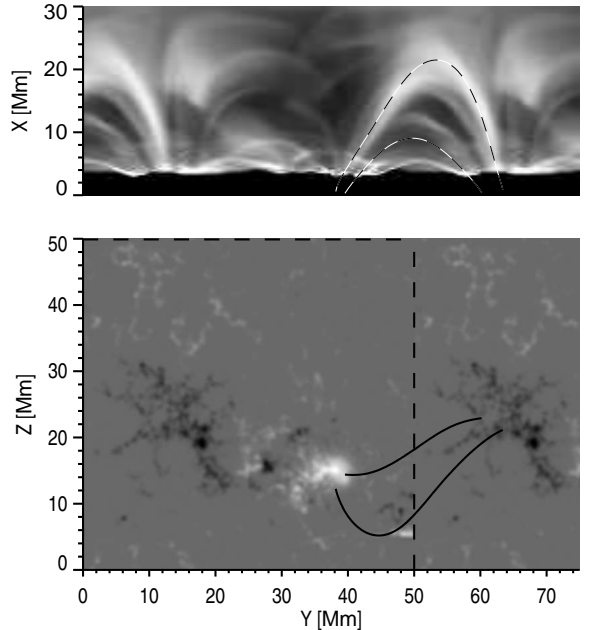


Fig. 2: Synthetic TRACE 171 emission measure, averaged over the z-direction, and raised to the power 0.5, to soften the contrast (top). SOHO/MDI magnetogram of AR 9114, used as initial condition, and the loops from Section 4 (bottom). One and a half box width is shown.

Slender loops of the type observed by TRACE in full size active regions are seen in this simulation as well (Fig. 2). They show that it is possible, merely by using a random photospheric convective velocity pattern, to create thin slender loops that do not expand much with height, and are almost isothermal, as required if they are to be observed in the narrow TRACE filters. Two loops have been followed; the first was selected for its brightness in the TRACE 171 filter and the second for its large electric current density. Their magnetic field line traces may be seen in Fig. 2, and their temperature, gas pressure and current helicity α have been plotted along the loops in Fig. 3. The loops both show a nearly constant pressure and temperature in the corona, maintained by the Spitzer conductivity forcing a small gradient in temperature along the loops. The winding number for the small loop is almost an order of magnitude larger than for the large loop, creating a level of heating that puts it outside the TRACE 171 filter, and thus renders it invisible in Fig. 2. Bright loops seen in the TRACE 171 filter generally have small winding numbers.

This suggests a scenario where loops are for a short period of time subjected to excess winding, which raises their chromospheric temperatures and evaporates mass (lowers the local height of the transition zone). The Spitzer conductivity maintains the coronal part of the loops close to isothermal, now with increased density and temperature. If the heating is only moderate, the individual loop may show up as bright in the TRACE 171 filter for a prolonged period, while if the heating is large the loop will pass through the TRACE 171 filter quickly, and will only be visible for a brief period of time. During this time these loops should be characterized by having large velocities along them, because of unbalanced pressure gradients.

Inspection of the arrangement of field lines along loops reveals an effect that is a likely explanation for the apparent lack of expansion with height of the slender loops. We find that a circular cross section at the top of loops is mapped to very flat

cross sections in the loop legs, presumably caused by the shearing motions in the photosphere. This, or even more complicated arrangement of field lines, is likely to explain why projected cross sections do not follow the naive $B^{-1/2}$ scaling expected for cross sections that remain circular.

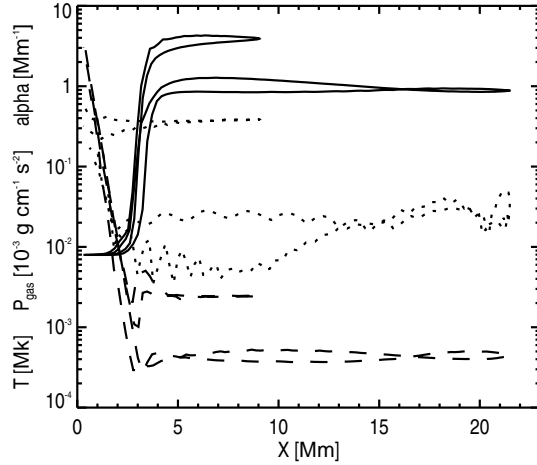


Fig. 3: Temperature (full line), gas pressure (dashed line), and current helicity ($\alpha = \mathbf{J} \cdot \mathbf{B} / B^2$ – dotted line) as a function of height x for the two loops traced in Fig. 2.

5. CONCLUSIONS

These initial investigations, to be followed by more detailed and extensive numerical experiments, have established that the DC (braiding) heating mechanism, originally proposed by Parker (1972), is effective and seems to be sufficient to heat the solar corona. Because of the very low plasma beta in the low corona above active regions, the dissipation of even a very small fraction of the non-potential magnetic energy is sufficient to heat the tenuous coronal plasma. The heating has a scale height behavior, consistent with the observational limits set by Aschwanden, Nightingale & Alexander (2000) for large scale coronal loops and by Aschwanden, Schrijver & Alexander (2001) for a range of loop sizes.

The results are not directly comparable to typical active re-

gions on the Sun, for three related reasons. First, the simulated region is small compared to typical solar active regions, which makes the loops correspondingly shorter. Second, the total simulated time is only about 40 minutes, corresponding to only a few turn-over times of the granular size part of the photospheric velocity field. This means that motions on larger scales, with much longer turn-over times, have yet only had little influence on the magnetic field, so large scale shears are still missing. Third, there is no emerging flux at the lower boundary, so part of the Poynting flux through the lower boundary is missing. Nevertheless, the results are tantalizing, and allows the identification of qualitative effects that are independent of these quantitative shortcomings.

The heating process automatically creates slender loops consistent with the ones seen in the solar corona by TRACE. These loops have, at the time when they show up in the emulated TRACE filter, almost constant temperature and density, and are not in hydrostatic equilibrium. The near uniform temperature is caused by the Spitzer conductivity forcing the loop to keep a small temperature gradient. The non-hydrostatic stratification is a signature of the fact that these loops are dynamic; they are caused by short duration excess heating, which causes up flows that increase the density along those magnetic field lines that are subjected to the excess heating. This defines the loop, and causes a selection effect; a loop will typically be observed when its density is near maximum, at which time it is by definition not in hydrostatic equilibrium. Even though the loops modeled here are shorter than the ones where deviations from hydrostatic equilibrium have been found observationally (Aschwanden, Schrijver & Alexander 2001), the same mechanism applies.

BVG acknowledges support through an EC-TMR grant to the European Solar Magnetometry Network. The work of ÅN was supported in part by the Danish Research Foundation, through its establishment of the Theoretical Astrophysics Center. Computing time at the Center for Parallel Computers, was provided by the Swedish National Allocations Committee. Both authors gratefully acknowledge the hospitality of LMSAL and ITP/UCSB (through NSF grant No. PHY99-07949) during this work.

REFERENCES

- Aschwanden, M.J. 2001, ApJ, 560, 1035
 Aschwanden, M.J., Nightingale, R.W., & Alexander, D. 2000, ApJ, 541, 1059
 Aschwanden, M.J., Schrijver, C.J., & Alexander, D. 2001, ApJ, 550, 1036
 Aschwanden, M.J., Tarbell, T.D., Nightingale, R.W., Schrijver, C.J., Title, A.M., Kankelborg, C.C., Martens, P., & Warren, H.P. 2000, ApJ, 535, 1047
 van Ballegooijen, A.A. 1986, ApJ, 311, 1001
 Berger, T.E., Löfdahl, M.G., Shine, R.A., & Title, A.M. 1998, ApJ, 506, 439
 Galsgaard, K., & Nordlund, Å. 1996 Journal of Geophysical Research 101, 13445–13460.
 Gomez, D.O., Dmitruk, P.A., & Milano, L.J. 2000, Sol. Phys., 195, 299
 Hathaway, D.H., Beck, J.G., Bogart, R.S., Khatri, G., Petitto, J.M., Han, S., & Raymond, J. 2000, Sol. Phys., 193, 299
 Hendrix, D.L., van Hoven, G., Mikić, Z., & Schnack, D.D. 1996, ApJ, 470, 1192
 Heyvaerts, J., & Priest, E.R. 1992, ApJ, 390, 297
 Kahn, F.D., 1976, A&A, 50, 145
 Longcope, D.W., & Sudan, R.N. 1994, ApJ, 437, 491
 Mikić, Z., Schnack, D.D., & van Hoven, G. 1989, ApJ, 338, 1148
 Nordlund, Å., & Galsgaard, K., 1995, technical report, Astronomical Observatory, University of Copenhagen
 Parker, E.N. 1972, ApJ, 174, 499
 Parker, E.N. 1983, ApJ, 264, 642
 Parker, E.N. 1988, ApJ, 330, 474
 Parnell, C.E., & Jubb, P.E. 2000, ApJ, 529, 554
 Schrijver, C.J., et al. 1999, Sol. Phys., 187, 261
 Schrijver, C.J., & Zwaan, C. 2000, Solar and Stellar Magnetic Activity, (Cambridge: University Press)
 Shine, R.A., Simon, G.W., & Hurlburt, N.E. 2000, Sol. Phys., 193, 393
 Spitzer, L., Jr. 1956, in Physics of fully ionized gases, (London: Interscience Publishers Ltd)
 Stein, R.F., & Nordlund, Å. 1998, ApJ, 499, 914
 Stein, R.F., & Nordlund, Å. 2000, Sol. Phys., 192, 91
 Sturrock, P.A., & Uchida, Y. 1981, ApJ, 246, 331
 Vernazza, J.E., Avrett, E.H., & Loeser, R. 1981, ApJS, 45, 635